Some preliminary results of a worldwide seismicity estimation: a case study of seismic hazard evaluation in South America

Theodoros M. Tsapanos (1) **and Cenka V. Christova** (2)
(1) *Aristotle University of Thessaloniki, Geophysical Laboratory, Thessaloniki, Greece*
(2) *Geophysical Institute, Bulgarian Academy of Science, Sofia, Bulgaria*

Abstract
Global data have been widely used for seismicity and seismic hazard assessment by seismologists. In the present study we evaluate worldwide seismicity in terms of maps of maximum observed magnitude (M_{max}), seismic moment (M_0) and seismic moment rate (M_0^{Σ}). The data set used consists of a complete and homogeneous global catalogue of shallow ($h \leq 60$ km) earthquakes of magnitude $M_S \geq 5.5$ for the time period 1894-1992. In order to construct maps of seismicity and seismic hazard the parameters a and b derived from the magnitude-frequency relationship were estimated by both: a) the least squares, and b) the maximum likelihood, methods. The values of a and b were determined considering circles centered at each grid point 1° (of a mesh 1°×1°) and of varying radius, which starts from 30 km and moves with a step of 10 km. Only a and b values which fulfill some predefined conditions were considered in the further procedure for evaluating the seismic hazard maps. The obtained worldwide M_{max} distribution in general delineates the contours of the plate boundaries. The highest values of M_{max} observed are along the circum-Pacific belt and in the Himalayan area. The subduction plate boundaries are characterized by the largest amount of M_0, while areas of continental collision are next. The highest values of seismic moment rate (per 1 year and per equal area of 10000 km^2) are found in the Southern Himalayas. The western coasts of U.S.A., Northwestern Canada and Alaska, the Indian Ocean and the eastern rift of Africa are characterized by high values of M_0^{Σ}, while most of the Pacific subduction zones have lower values of seismic moment rate. Finally we analyzed the seismic hazard in South America comparing the predicted by the NUVEL1 model convergence slip rate between Nazca and South America plates with the average slip rate due to earthquakes. This consideration allows for distinguishing between zones of high and low coupling along the studied convergence plate boundary.

Key words *seismicity – maximum observed magnitude – seismic moment – seismic momente rate – V3/V1 – V1-V3*

1. Introduction

Quantitative methods have been applied over the years to estimate seismicity and seismic hazard. The most common seismic parameter analyzed is the magnitude of earthquakes and numerous studies (Kaila and Narain, 1971; Yegulap and Kuo, 1974; Ryall and van Wormer, 1980; Makropoulos and Burton, 1985; Rundle, 1989; Schwartz and Coppersmith, 1989; Tsapanos and Burton, 1991; Pacheco and Sykes, 1992) among others, have focused on this parameter. Quantities that can be considered measures of seismicity are the number of events above a certain magnitude threshold, the slope of Benioff graph, the M_{max} observed, etc.

Maps of seismicity in their simplest form represent the past historic and/or instrumentally recorded seismicity of a region, the intensity

Mailing address: Dr. Theodoros M. Tsapanos, Aristotle University of Thessaloniki, Geophysical Laboratory, GR 54006 Thessaloniki, Greece; e-mail: tsapanos@geo.auth.gr

distributions or contours of elastic energy release. In constructing such maps it is assumed that future seismicity will be the same as past activity. Such an assumption is true only if the data set is complete for a long period compared to the recurrence time of the slowest moving fault in a region and only in this case will such map accurately present the long-term hazard. In practice, the above condition is rarely met. Maps constructed without taking into account the above may represent a misleading picture of present-day hazard. Quiet zones of such map, *i.e.* of low hazard, may delineate seismic gaps and actually be places of high hazard. On the other hand, zones that recently have experienced large earthquakes, and are characterized by high hazard on the map may actually be places of low hazard in the near future. Therefore the two main problems with such maps are: 1) incompleteness of the geographical and temporal coverage in record, and 2) a lack of identification of a time datum upon which to base the hazard estimation (Scholz, 1994).

The first problem can be solved by incorporating geological data on fault slip rates (*e.g.*, Allen, 1975; Wesnousky *et al.*, 1984) or by using the developed by Molnar (1979) formalism for determining the frequency of the occurrence of earthquakes. This formalism incorporates information about the relative frequency of earthquakes occurrence and the average rate of slip as well as consideration of more general geometries than a single fault.

The aim of the present study is mainly to compile global seismicity maps, incorporating a complete and homogeneous data set and different seismological parameters (M_{max} observed, M_0 and seismic moment rates). The method used allows presentation of both local and regional variation of the seismic hazard. These maps effectively produce a brief atlas of seismicity.

2. Data used and method applied

A global homogeneous catalogue of earthquakes compiled by Tsapanos *et al.* (1990) with magnitudes $M_s \geq 5.5$ covering a time span of 98 years (1894-1990) was used. This catalogue was recently improved by considering the magnitudes given by Pacheco and Sykes (1992). The data of the years 1991 and 1992 were extracted from the bulletins of ISC. The completeness of this catalogue was secured by dividing the whole period into four subperiods, choosing for each of them a proper minimum earthquake magnitude and the whole procedure was statistically checked by Papazachos *et al.* (1990). The four subperiods and the corresponding magnitude thresholds are: a) 1894-1992, $M_s \geq 7.0$; b) 1930-1992, $M_s \geq 6.5$; c) 1953-1992, $M_s \geq 6.0$, and d) 1966-1992, $M_s \geq 5.5$. We have dealt with shallow ($h \leq 60$ km) earthquakes only. A map which depicts the spatial distribution of epicenters of earthquakes used in the present study is demonstrated in fig. 1.

The parameters currently used for quantitative evaluation of seismicity are the well known a and b derived from the magnitude-frequency relationship (Gutenberg and Richter, 1944).

$$\log N(M) = a_t - bM \tag{2.1}$$

The a value reduced to 1 year was also obtained

$$a = a_t - \log t. \tag{2.2}$$

From eqs. (2.1) and (2.2) we obtained for a 1 year period

$$\log N(M) = a - bM. \tag{2.3}$$

The reliable estimation of parameters a and b is of primary importance because the evaluation of seismicity in our study depends on them. The method used for the estimation of these parameters is based on the one described in Tsapanos and Papazachos (1998). According to this technique the whole world is divided into a grid point mesh $1° \times 1°$. The values of a and b are estimated for each grid point by a least squares method according to the relations (2.1) and (2.2) and using data of earthquakes located inside circles centered at the point. In order to ensure reliable b-value estimates the following conditions (Hatzidimitriou *et al.*, 1994; Tsapanos and Papazachos, 1998), under which the obtained b- values are acceptable:

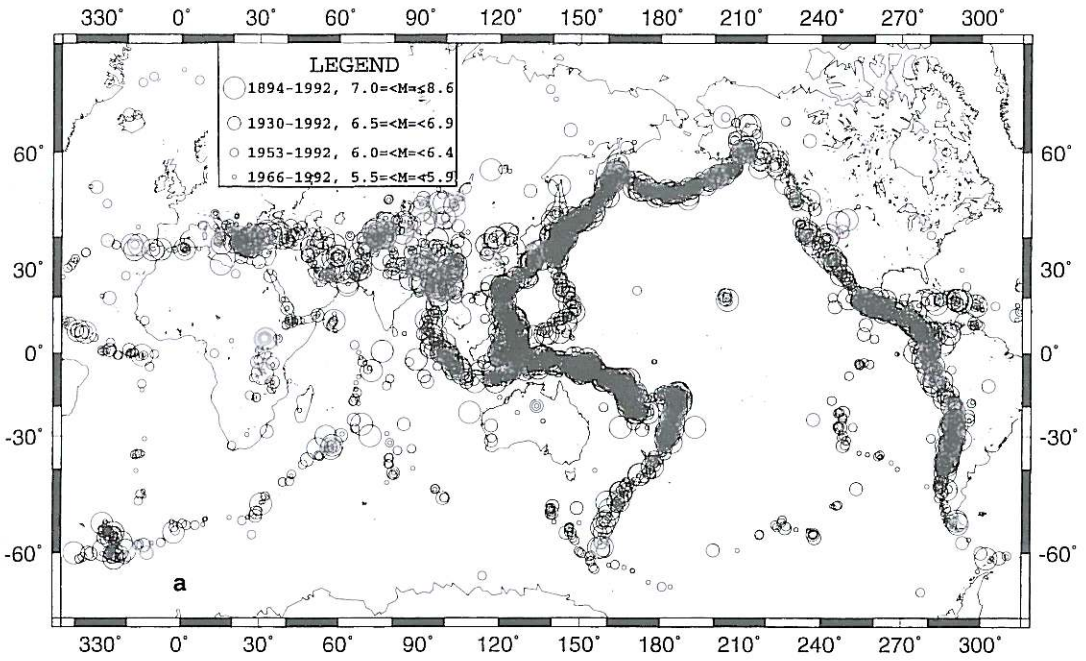

Fig. 1. A worldwide geographical distribution of the epicenters of shallow earthquakes used in the present study. The data are depicted in accord with their completeness (after Tsapanos and Papazachos, 1998).

1) The number of epicenters in the circles are 15 or larger.

2) The number of points in the Log*N*-*M* plot are 5 or larger.

3) The difference between the maximum and the minimum magnitude of earthquakes in the circle is equal or larger than 1.5 (Papazachos, 1974).

The radius of the circles varies, with a step of 10 km, until it reaches a value at which the above conditions are fulfilled. In very few extreme cases (areas with rare occurrence of earthquakes) the circle radius reaches 500 km. By this procedure we estimated the *b*-value with uncertainty for 12 regions in the world. The results are listed in table I.

Another approach to estimate the *b*-values is given by Kijko and Sellevoll (1989). They used the maximum likelihood method for evaluating the seismic parameters of earthquakes activity rate λ and *b*-value, $\Theta = (\lambda, \beta)$. Putting $\partial \ln L(\Theta \mid X)/\partial\lambda = 0$ and $\partial \ln L\ (\Theta \mid X/\partial\beta = 0$, after the calculations we can obatin

$$\frac{1}{\lambda} = \phi_1^E + \phi_1^C \tag{2.4}$$

and

$$\frac{1}{\beta} = \langle X \rangle - \phi_2^E - \phi_2^C + \lambda[\phi_3^E + \phi_3^C\ ] \tag{2.5}$$

the full description of the above functions is given in Kijko and Dessokey (1987) and Kijko and Sellevoll (1989). After cumbersome computations eq. (2.5) becomes

$$\frac{1}{\beta} = \langle X \rangle - \frac{\langle tX_0 A \rangle - \langle t \rangle A_2 m_{\max}}{\langle tA \rangle - \langle t \rangle A_2} \tag{2.6}$$

were we have

$$\langle t \rangle = \sum t_i / n_0,$$

$$\langle tA \rangle = \sum t_i \cdot A(X_{0i}) / n_0,$$

Table I. The regional mean b values with the uncertainty estimated for 12 regions of the world.

Regions	$b \pm$ uncertainty	
	Least squares	Max. likelihood
South America	0.81 ± 0.17	0.79 ± 0.02
Middle America and Mexico	0.75 ± 0.15	0.72 ± 0.03
West coasts of North America and Canada	0.76 ± 0.15	0.70 ± 0.05
Caribbean Loop	0.80 ± 0.13	0.77 ± 0.06
Alaska and Aleutian islands	0.85 ± 0.20	0.88 ± 0.02
Kamchatka-Kuril islands and Japan	0.80 ± 0.20	0.93 ± 0.03
Mariannes islands	0.85 ± 0.17	0.97 ± 0.05
Philippines islands	0.79 ± 0.15	0.79 ± 0.05
Sunda arc	0.82 ± 0.12	0.84 ± 0.02
Guinea to New Hebrides islands	0.83 ± 0.17	0.79 ± 0.02
Fiji, Tonga, Kermadec and N. Zealand islands	0.84 ± 0.18	0.81 ± 0.02
Eurasia continent	0.77 ± 0.16	0.76 ± 0.05
Mean	0.806 ± 0.04	0.811 ± 0.07

and

$$\langle tX_0 A \rangle = \sum t_i \cdot X_{0i} \cdot A(X_{0i}) / n_0$$

where the summation is from $i = 1, ..., n_0$ and $\langle X \rangle$ is equal to the mean earthquake magnitude estimated from the extreme and complete part of a catalogue, $n = \Sigma_{i=0} n_i$ is the total number of earthquakes, and $r_i = n_i/n$.

Equation (2.6) can be used for maximum likelihood estimation of β in the case when input data are limited to maximum magnitudes taken from unequal time intervals. It is then easy to calculate b-values, given that the parameter β is interrelated to b with the equation $b = \beta \log e$. The b-value (illustrated in table I) with the uncertainty was then computed through the approach of maximum likelihood for 12 regions of the world. It is interesting that though the regional values of b obtained by the two approaches used are not always equal, their mean b-values are almost equal to 0.81. Chouhan (1970) proposed a global b-value equal to 0.80. An unbiased estimator with the lowest possible variance and a Bayesian one were considered by Pisarenko *et al.* (1996) in order to estimate seismic hazard in California and Italy.

Also Kijko (1988) suggested a new procedure for the evaluation of the maximum regional magnitude $M_{\max}^{\text{reg}}$ which is based on the equation that compares the largest observed magnitude $M_{\max}$ and the maximum expected magnitude $E(M_{\max}^{\text{reg}} / T)$ during the span T of a catalogue. The estimator of maximum regional magnitude is given by the following equation:

$$M_{\max}^{\text{reg}} = M_{\max} + \frac{E_1(TZ_2) - E_1(TZ_1)}{\beta \exp(-TZ_2)} - \tag{2.7}$$

$$-M_{\min} \exp(-\lambda T).$$

The quantities in eq. (2.7) are computed as: $Z_1 = \lambda A_1/(A_1 - A_2)$, $Z_2 = \lambda A_2/(A_1 - A_2)$, $A_1 = \exp(-\beta M_{\min})$, $A_2 = \exp(-\beta M_{\max})$ and $E_1(\cdot)$ denotes an exponential integral function (Abramowitz and Stegum, 1970)

$$E_1(z) = \int_z^{\infty} \exp(-\zeta) / \zeta d\zeta. \tag{2.8}$$

Based on the above procedure we evaluated the earthquakes hazard of the regions which are listed in table I. Figure 2a,b illustrates the mean

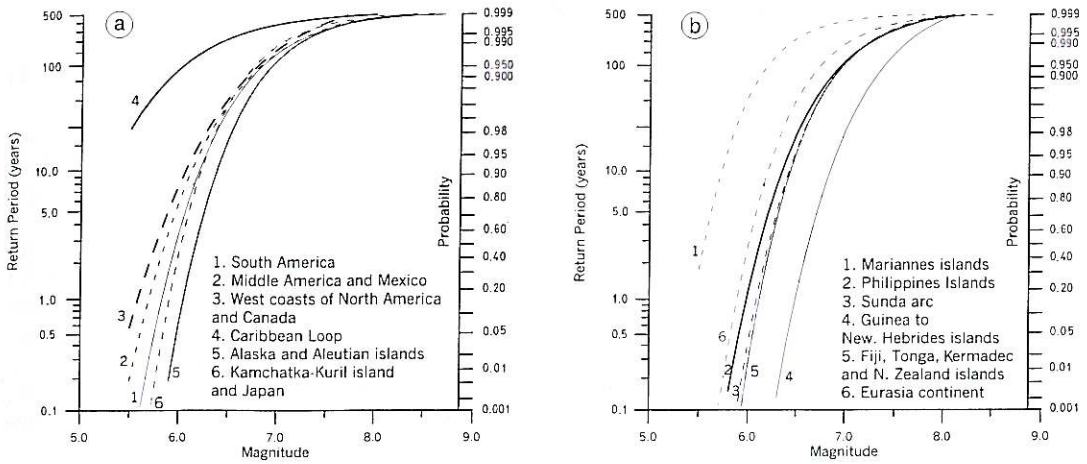

Fig. 2a,b. The return period/probability/magnitude diagram: a) for regions of South America, Middle America and Mexico, West coasts of North America and Canada, Caribbean Loop, Alaska and Aleutian islands and Kamchatka-Kuril islands-Japan, and b) Mariannes islands, Philippines islands, Sunda arc, Guinea to New Hebrides islands, Fiji, Tonga, Kermadec and New Zealand and Eurasia continent.

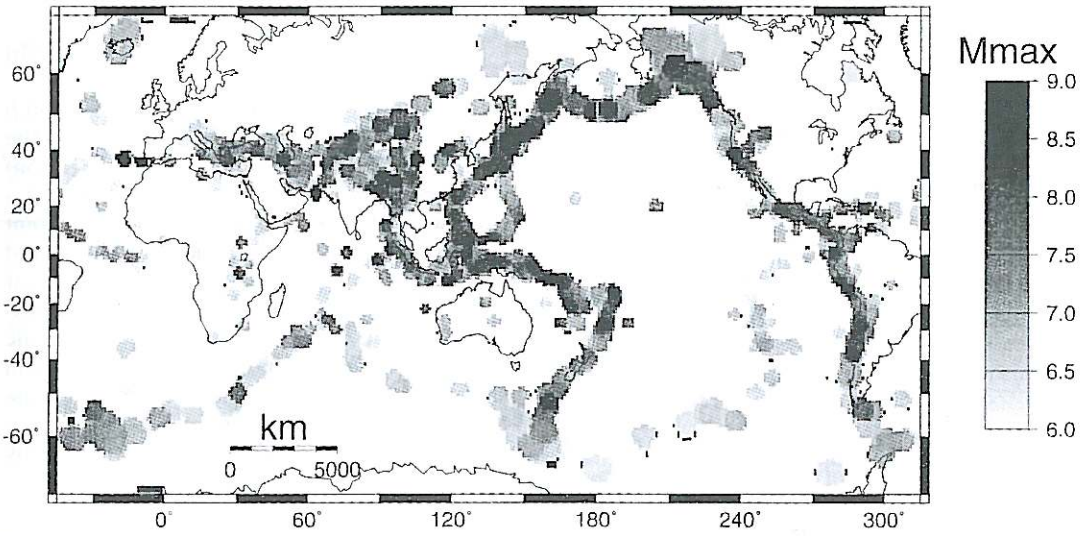

Fig. 3. A global seismic hazard map in terms of the maximum observed magnitude M_{max}.

return periods and the probability that a certain magnitude will not be exceeded in any year for the examined regions.

Maximum magnitude is the term given for the upper limit truncation of the magnitude-frequency distribution employed in defining a specific seismic source or region. In the present case the observed maximum magnitude (which is the maximum ever recorded) was evaluated for each 1° point. This quantity deduced direct-

ly from the data processing, is considered a measure for seismicity assessment. In fig. 3 we have plotted in a global scale the observed M_{max}. The seismicity is efficiently expressed through this map. Places of high or low seismicity are represented by their own M_{max} which is characteristic for each one.

3. Evaluation of seismic moment and seismic moment rates

It is well known that the surface wave magnitudes M_s are saturated when they reach the value of about 8.0 (Heaton *et al.*, 1986). Therefore it is useful to measure the «size» of earthquakes in terms of the seismic moment instead. The seismic moment M_0 describes the static aspects of earthquake. A relation similar to Gutenberg and Richter's (1944), can be derived for seismic moment by applying the empirical relation (Kanamori, 1977)

$$\log N(M_0) = cM + d. \qquad (3.1)$$

In accord with Molnar (1979) if we combine eqs. (2.3) and (3.1) we obtain

$$\log N(M_0) = a + \frac{bd}{c} - \frac{b}{c}\log M_0 \qquad (3.2)$$

where $N(M_0)$ is now the number of events with seismic moment greater or equal to M_0, which can be written as

$$N(M_0) = \alpha M_0^{-\beta} \qquad (3.3)$$

where $\alpha = 10^{(a+bd/c)}$ and $\beta = b/c$. It is well known that for each region of the Earth a maximum magnitude M_{max} exists or a maximum seismic moment M_0^{max} above which no earthquakes occur.

The total seismic moment M_0^{Σ} that is accumulated for a long time τ in a region can be estimated from $M_0^{\Sigma} = \dot{M}_0^{\Sigma}\tau = \mu A\bar{u}\tau$, where $\dot{M}_0^{\Sigma}$ is the rate of occurrence of seismic moment, μ is the shear modulus and $\bar{u}$ is the average slip exluding creep (Brune, 1968). The seismic moment rate in a region is estimated according to Brune's (1968) formulation and is

$$\dot{M}_0^{\Sigma} = \frac{\alpha}{1-\beta} M_0^{max\,1-\beta} \qquad (3.4)$$

where $\alpha = 10^{(a+b16.14/1.5)}$, $\beta = b/1.5$, the a-parameter is estimated from eq. (2.3) while the b-values are adopted from both eqs. (2.3) and (2.6) and the mean regionals b are taken into account.

In the catalogue adopted, we use M_s instead of M_w (Kanamori's moment magnitude M_w, 1977) because M_s is generally considered to correlate best with seismic moment (Ekström and Dziewonski, 1988). In order to compute the maximum seismic moment we used the global average relationship derived by Ekström and Dziewonski (1988)

$$\log M_0 = 30.20 - \sqrt{92.45 - 11.40 M_s}, \quad \text{for } 5.3 \le M_s \le 6.8 \qquad (3.5a)$$

and

$$\log M_0 = 16.14 + \frac{3}{2} M_s, \quad \text{for } M_s > 6.8 \qquad (3.5b)$$

Incorporating the obatined estimates of a and b and the M_{max} observed we evaluated further the seismic moments (M_0) by the use of eqs. (3.5a) and (3.5b) and the seismic moment rates ($\dot{M}_0^{\Sigma}$) from eq. (3.4) in the same $1° \times 1°$ grid point mesh. Both quantities, which can be considered measures of seismicity, are evaluated per 1 year and per equal area of 10 000 km^2. The constructed maps of the global distribution of seismic moment and seismic moment rate are shown in figs. 4 and 5, respectively. Similar maps of distribution of seismic moment released on a global basis from 1900 to 1989 are presented by Pacheco and Sykes (1992).

4. Brief comments on the obtained results

The map of seismicity expressed in terms of M_{max} in shown in fig. 3. A general feature observed in fig. 3 is that M_{max} delineates the plate boundaries. Very large values are focused in places which experienced large earthquakes in the present century, like Chile, California,

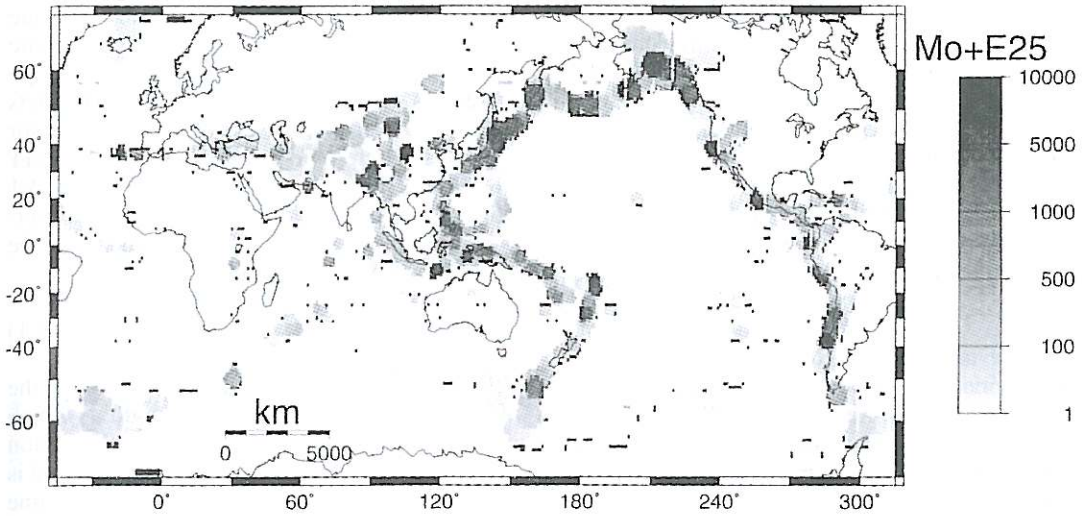

Fig. 4. A global seismic hazard map in terms of the seismic moment M_0. It is expressed in (dyne·cm $\times 10^{25}$).

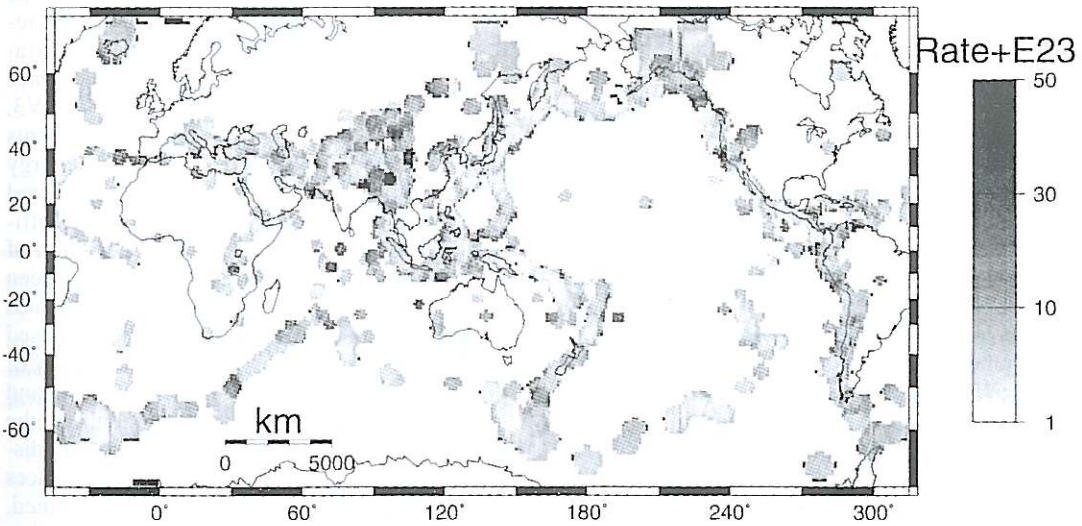

Fig. 5. A global seismic hazard map in terms of seismic moment rate M_0^{Σ}. It is expressed in $\left(\frac{\text{dyne}\cdot\text{cm}}{\text{yr}}\times 10^{23}\right)$.

Alaska, Aleutian islands, Northern Japan, Tonga island and Sunda arc, all of them bound to the circum Pacific belt. Only two very large values of M_{max} are observed in the Eurasian belt, both related to the Himalayan tectonics. Large values of the parameter M_{max} are well defined along the plate boundaries of the circum Pacific. Large values of the M_{max} are also depicted in Pakistan, Iran, Turkey and Greece, all belonging to the Eurasian belt.

Another measure of seismicity is the seismic moment. Following the theoretical background discussed in the previous section, we evaluated further the seismic moment M_0 (in dyne × cm × × 10^{25}) in a 1°×1° grid and based on M_{max} observed. The global seismicity expressed through M_0 is illustrated in the map of fig. 4 which is a worldwide distribution of seismic moment. A similar map was compiled by Pacheco and Sykes (1992). However, they considered earthquakes of $M_s \geq 7.0$ only while our catalogue data are complete for $M_s \geq 5.5$. This is why we believe that our map is more detailed than theirs. A characteristic feature in fig. 4 is the very large value of M_0 in Chile where the largest earthquakes of the present century with M_w = 9.5 (Kanamori, 1977) occurred. The same value is observed in Tibet which experienced two giant earthquakes in 1920 with M_s = 8.4 and in 1950 with M_s = 8.6. In both places, Chile and Tibet, the estimated seismic moment reaches 10000 × 10^{25} dyne × cm. Places of high M_0 are found in Northern Chile, Peru, Alaska, Aleutian islands, Kamchatka and Northern Japan, Indonesia, Tonga and Kermadec islands in the circum Pacific. The largest amount of seismic moment is observed along the plate boundaries of subduction type, while areas of continental collision are next. Fracture zones and oceanic ridges (mid-oceanic tectonic system) are characterized by small values of seismic moment.

The third map (fig. 5) illustrates the worldwide seismic moment rate (in dyne × cm/yr × × 10^{23}). Very high values of M_0^{Σ} are observed in the Southern Himalayas. High values are depicted in the Western U.S.A., Northwestern Canada and Alaska, around the Himalayas, Pakistan, in the Indian Ocean and in the eastern rift of Africa. It is interesting that most of the Pacific subduction zone are characterized by lower values of seismic moment rate.

5. Seismic hazard evaluation in South America

In this section we attempt to evaluate the seismic hazard in South America comparing the NUVEL1 model predicted convergence slip rate between the Nazca and the South America plates (DeMets *et al.*, 1990) with the average slip rate due to earthquakes. The motion of the tectonic plates Nazca and South America (NUVEL1 model) is described by 99 slip vectors (DeMets *et al.*, 1990) from the Chile, Peru and Equator trenches, where 68 of them derived from CMT solutions. These slip vectors are marked as V1 for the purpose of the present study. The average seismic slip due to an earthquake can be estimated from the relationship

$$M_0 = \mu A \bar{v} \qquad (5.1)$$

(Brune, 1968; Molnar, 1979), where M_0 is the seismic moment, μ is the shear modulus which is 3.3×10^{11} dyne·cm^2, A the area of the region $L \times W$ (length and width, respectively) and $\bar{v}$ is the average slip. M_0 is evaluated per unit time (1 year) and we can assume that $\bar{v}$ is considered the average slip rate. We applied all the above referred equations for South America and finally we evaluated the $\bar{v}$, which hereafter will be called V3. We estimated V3 for cells corresponding to those of V1 in order to be comparable. In further analysis we consider the space distribution of the quantities V3/V1 and V1-V3. The first of these quantities (V3/V1) represents the percentage of the plate movement energy released by earthquakes. It could be considered an expression of the seismic coupling coefficient (Scholz, 1994). The space distribution of the second one (V1-V3) distinguishes between places where the interaction between two plates occurs through earthquakes from those caused by mostly creep. The results of the case study of South America shows that maps of V3/V1 and V1-V3 give additional information about the seismic hazard. Figure 6 shows the spatial distribution of V3/V1 in South America. Two places (1 and 2) of high V3/V1 values are outlined. These places are related to the large earthquakes of 1960 (M_s = 8.5) and of 1942 (M_s = 8.0), respectively. The results indicate that although places 1 and 2 are characterized by strong coupling between Nazca and South America, the coupling in place 1 (V3/V1 ≈ 8) is almost twice the coupling in place 2 (V3/V1 ≈ 4.5). Ruff and Kanamori (1980) suggested such a strong coupling, but for the whole Nazca underthrusting area. Also Tajima and Kanamori (1985) sug-

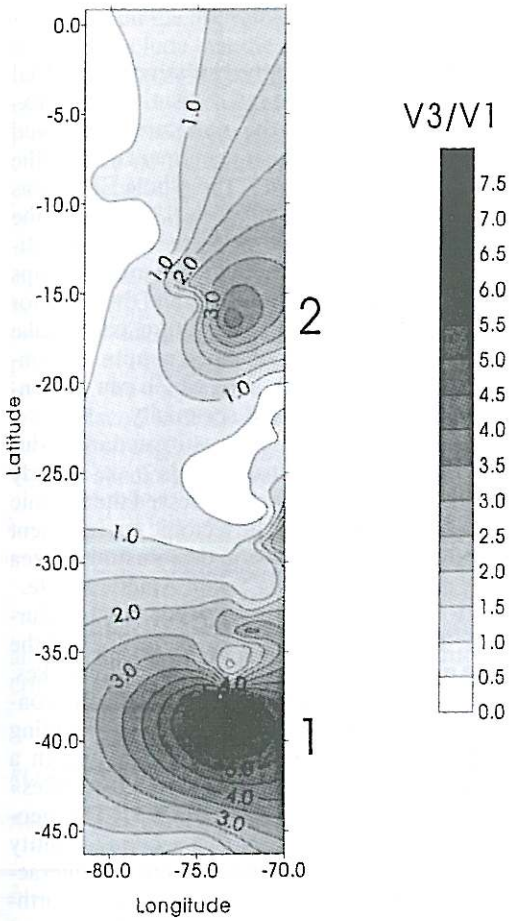

Fig. 6. Seismic hazard in South America as expressed through the quantity V3/V1 which represents the percentage of the plate movement energy released by earthquakes.

gested that the degree of coupling controls the scale-length of heterogeneities presented in the plate interface; while Davis and Frohlich (1991) suggested that strong coupling results in fewer heterogeneities and large earthquakes. When V3/V1 is 1.0 we have full coupling between the two plates while values of V3/V1 close to 0.0. indicate aseismic coupling. However, the values of the V3/V1 ratio are higher than 1.0 over places 1 and 2. This is due to the fact that for estimating the value of V3 we dealt with data coverage of 98 years only, which is shorter than the return period of large earthquakes ($M_s > 8.0$). The estimate for the recurrence time of such large earthquakes ranges between 130 and 400 years (Rikitake, 1976; Nishenko, 1991; Scholz, 1994). Bearing this in mind our results help to make the following conclusions. The first is that all the energy released in place 1 is due to the plate convergence which «goes» for genesis of earthquakes, *i.e.* the two plates are fully coupled there, while the same exists in place 2 but the coupling here is half of that in place 1, and secondly that the time coverage of our data is short enough. Other places of high values of V3/V1 are –28°/–70° where an event of $M_s = 8.1$ occurred in 1922, and –33.6°/–72.0°N where in 1906 an earthquake of $M_s = 8.0$ released. Therefore our results indicate that places of high values of V3/V1 and very high seismic moment (rate) are to be related to both insufficient time coverage of the data used and to strong seismic coupling between the converging Nazca and the South America plates. On the other hand, places of low seismic moment (rate) and very low values of V3/V1 (close to 0.0) could be due either to the short time period considered or to aseismic coupling between the converging plates.

The spatial distribution of V1-V3 for South America is demonstrated in fig. 7. Zones of positive values of V1-V3 are places where part of the plate movement energy is released by aseismic slip. In places of negative values of V1-V3 the plate convergence energy is released by earthquakes. Therefore such places may be considered places of high hazard. Nishenko (1991) suggested that the amount of aseismic slip in area (place) 1 is insignificant, and that almost all of the tectonic energy «goes» into the occurrence of large shocks. This is in good agreement with our results. Place 1, where the great Chilean earthquake occurred in 1960, has the highest seismic hazard in terms of V1-V3 (= –550.0) value. This indicates that almost all of the energy due to the plate convergence was released by a large earthquake. For this place Sykes and Quittmeyer (1981) found that the total plate velocity is 9.1 cm/yr, the convergence plate velocity is 8.6 cm/yr and the slip displacement is 18.71 cm. Another place of high seismic

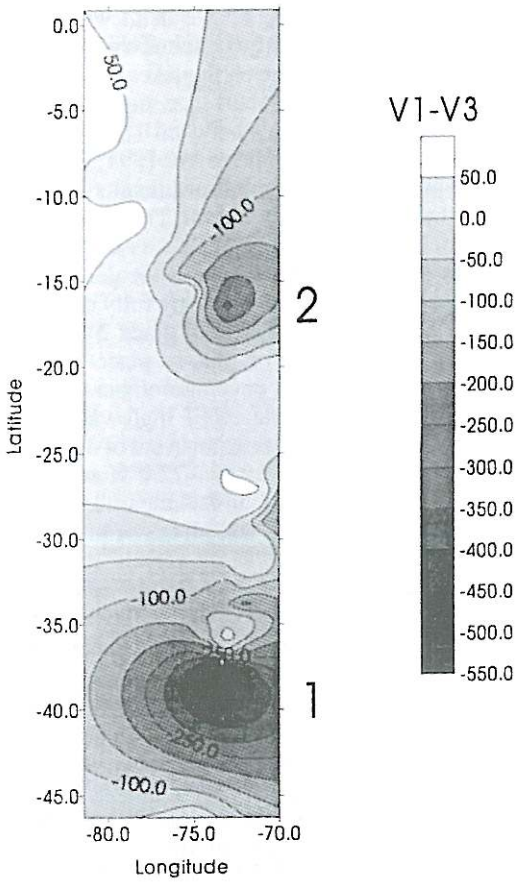

Fig. 7. Seismic hazard in South America as expressed through the quantity V1-V3. Its spatial distribution distinguishes between places where the interaction between two plates occurs through earthquakes from those caused by mostly creep.

hazard (but less than that of place 1) is depicted in place 2, where the intersection of the Nazca ridge into South America forms an active area for large shocks (Nishenko, 1985). Here the obtained values of V1-V3 (= −263.0) could be due to the lower total plate velocity which is in accord to Sykes and Quittmeyer (1981) is 8.7 cm/yr, while the convergent plate velocity is 8.2 cm/yr. A place of lower seismic hazard value is located between latitudes −20°S and −26°S.

6. Summary and discussion

A detailed study on the assessment of global seismicity was carried out. Seismicity was expressed in terms of the maximum observed magnitude M_{max}, the seismic moment M_0 and the seismic moment rate M_0^{Σ}. The whole Earth was divided into grid point mesh 1°×1° and the seismicity expressed through the three quantities is estimated for each 1°. Seismicity maps are always working documents and the basis for provisional judgements on future earthquake activity. Based on the obtained results we constructed three detailed maps which can be considered as atlas of global seismicity.

Seismic hazard was also estimated individually for South America. This is a case study because we evaluated and expressed the seismic hazard as a function of the tectonic environment of the area, which is the underthrusting Nazca plate and the overriding South America plate.

Two quantities were derived for this purpose. The first represents the percentage of the plate movement energy released by earthquakes, and according to Scholz (1994) could be considered an expression of the seismic coupling coefficient. When we have full coupling in a place it is characterized by «fast earthquakes» and *vice versa* (Muir-Wood, 1993). The geographical distribution of the second quantity distinguishes between areas where the interaction between the two plates results in earthquakes from those where aseismic slip (creep) mostly occurs.

Two places of particular interest were found. The local characteristic tectonic features of these places are the intersections of the Mocha fracture zone for the former and the Nazca ridge for the latter. Place 1, characterized by very high V3/V1, high seismic moment and low V1-V3, is related to the place of the large Chilean earthquake of 1960 (M_s = 8.5). The values of V3/V1, V1-V3 and seismic moment over place 2, which correlates with the large earthquake of 1942 (M_s = 8.0), are also high but twofold less than these of place 1. According to previous studies, place 1 is characterized by negligible aseismic slip and by shorter recurrence time for large earthquakes than place 2 (*e.g.*, Nishenko 1985, 1991).

Based on the above observations and results we can conclude that the two places 1 and 2 are of different seismic hazard behavior: place 1 is indicated to have higher seismic hazard than place 2. According to Nishenko (1985) the recurrence time for large earthquakes is 100-167 years in place 1 and 111-296 years in place 2. In fast plate boundary interface the hazard is high, while in slow parts of plate boundaries, where earthquakes rarely occurred the seismic hazard is low (Muir-Wood, 1993). Therefore we can conclude that place 1 (where we have full coupling) is of high seismic hazard and is characterized by the recurrence of «fast» earthquakes, while place 2 is of lower seismic hazard (though it is in strong coupling plates interface) and «slow» shocks are retrieved there.

Acknowledgements

The authors are grateful to Dr. V. Pisarenko and the anonymous reviewer for constructive criticism of the manuscript.

REFERENCES

ABRAMOWITZ, M. and I.R. STEGUM (1970): *Handbook of Mathematical Functions* (Dover Publ., New York), 9th edition, pp. 1046.

ALLEN, C.R. (1975): Geological criteria for evaluating seismicity, *Bull. Seismol. Soc. Am.*, **86**, 1041-1057.

BRUNE, J.N. (1968): Seismic moment, seismicity and rate of slip along major fault zones, *J. Geophys. Res.*, **73**, 777-784.

CHOUHAN, R.K.S. (1970): On the frequency-magnitude relation log$N$ = a-bM, *Pageoph*, **81**, 119-123.

DAVIS, S.D. and C. FROHLICH (1991): Single-link cluster analysis of earthquake aftershocks: decay laws and regional variations, *J. Geophys. Res.*, **96**, 6335-6350.

DEMETS, C., R.G. GORDON, D.F. ARGUS and S. STEIN (1990): Current plate motions, *Geophys. J. Int.*, **101**, 425-478.

EKSTRÖM, G. and A.M. DZIEWONSKI (1988): Evidence of bias in estimations of earthquake size, *Nature*, **332**, 319-323.

GUTENBERG, B. and C.F. RICHTER (1944): Frequency of earthquakes in California, *Bull. Seismol. Soc. Am.*, **34**, 185-188.

HATZIDIMITRIOU, P.M., B.C. PAPAZACHOS and G.F. KARAKAISIS (1994): Quantitative seismicity of the Aegean and surrounding area, in *Proceedings XXIV General Assembly ESC, Athens, Greece 19-24 September 1994*, vol. 1, 155-164.

HEATON, T.H., F. TAJIMA and A.W. MORI (1986): Estimate ground motion using recorded accelerograms, *Surv. Geophys.*, **8**, 25-83.

KAILA, K.L. and H. NARAIN (1971): A new approach for preparation of quantitative seismicity maps as applied to Alpide belt - Sunda arc and adjoining areas, *Bull. Seismol. Soc. Am.*, **61**, 1275-1291.

KANAMORI, H. (1977): The energy release in great earthquakes, *J. Geophys. Res.*, **82**, 2981-2987.

KIJKO, A. (1988): Maximum likelihood estimation of Gutenberg-Richter b parameters for uncertain magnitudes values, *Pageoph*, **127**, 573-579.

KIJKO, A. and M.M. DESSOKEY (1987): Application of the extreme magnitude distributions to incomplete earthquake files, *Bull. Seismol. Soc. Am.*, **77**, 1429-1436.

KIJKO, A. and M.A. SELLEVOLL (1989): Estimation of seismic hazard parameters from incomplete data files. Part I. Utilization of extreme and complete catalogs with different threshold magnitudes, *Bull. Seismol. Soc. Am.*, **79**, 645-654.

MAKROPOULOS, K.C. and P.W. BURTON (1985): Seismic hazard in Greece: I. Magnitude recurrence, *Tectonophysics*, **117**, 205-257.

MOLNAR, P. (1979): Earthquake recurrence intervals and plate tectonics, *Bull. Seismol. Soc. Am.*, **69**, 115-133.

MUIR-WOOD, R. (1993): From global seismotectonics to global seismic hazard, *Ann. Geofis.*, **34** (3-4), 153-168.

NISHENKO, S.P. (1985): Seismic potential for large and great interplate earthquakes along the Chilean and Southern Peruvian margins of South America: a quantitative reappraisal, *J. Geophys. Res.*, **90**, 3589-3615.

NISHENKO, S.P. (1991): Circum-Pacific seismic potential: 1989-1999, *Pageoph*, **135**, 169-259.

PACHECO, J.F. and L.R. SYKES (1992): Seismic moment catalog of large shallow earthquakes, 1900 to 1989, *Bull. Seismol. Soc. Am.*, **82**, 1306-1349.

PAPAZACHOS, B.C. (1974): Dependence of the seismic parameter b on the magnitude range, *Pageoph*, **112**, 1059-1065.

PAPAZACHOS, B.C., T.M. TSAPANOS, E.M. SCORDILIS, C.B. BAGIATIS and CH.C. KOUKOUVINOS (1990): Evidence for a stochastic model of global seismicity, in *Proceedings 5th Congress of the Geological Society of Greece, 24-27 May, Thessaloniki, Greece*, **25** (3), 205-216.

PISARENKO, V.F., A.A. LYUBUSHIN, V.B. LYSENKO and T.V. GOLUBEVA (1996): Statistical estimation of seismic hazards parameters: maximum possible magnitude and related parameters, *Bull. Seismol. Soc. Am.*, **86**, 691-700.

RIKITAKE, T. (1976): Recurrence of great earthquakes at subduction zones, *Tectonophysics*, **35**, 335-362.

RUFF, L. and H. KANAMORI (1980): Seismicity and the subduction process, *Phys. Earth Planet. Inter.*, **23**, 240-252.

RUNDLE, J.B. (1898): Derivation of the complete Gutenberg-Richter magnitude-frequency relation using the principle of scale invariance, *J. Geophys. Res.*, **94**, 12337-12342.

RYALL, A.S. and J.D. VAN WORMER (1980): Estimation of maximum magnitude and recommended seismic zone

changes in the western great basin, *Bull. Seismol. Soc. Am.*, **70**, 1573-1581.

SCHOLZ, C.H. (1994): *The Mechanics of Earthquakes and Faulting* (Cambridge Univ. Press), pp. 439.

SCHWARTZ, D.P. and K.J. COPPERSMITH (1989): Fault behavior and characteristic earthquakes: example from the Wasatchand and the San Andreas fault zones, *J. Geophys. Res.*, **89**, 5681-5698.

SYKES, L.R. and R.C. QUITTMEYER (1981): Repeat times of great earthquakes along simple plate boundaries, in *Earthquake Prediction, an International Review*, edited by D.W. SIMPSON and P.G. RICHARDS, *Maurice Ewing Series*, Washington D.C., **4**, 217-247.

TAJIMA, F. and H. KANAMORI (1985): Aftershock area expansion and mechanical heterogeneity of fault zones within subduction zone, *Geophys. Res. Lett.*, **12**, 345-348.

TSAPANOS, T.M. and P.W. BURTON (1991): Seismic hazard evaluation for specific seismic regions of the world, *Tectonophysics*, **194**, 153-169.

TSAPANOS, T.M. and B.C. PAPAZACHOS (1998): Geographical and vertical variation of the Earth's seismicity, *J. Seismol.*, **2**, 183-192.

TSAPANOS, T.M., E.M. SCORDILIS and B.C. PAPAZACHOS (1990): A global catalogue of strong ($M_s \geq 5.5$) earthquakes during the time period 1897-1985, *Publ. Geophys. Lab., Univ. of Thessaloniki*, **10**, pp. 90.

WESNOUSKY, S., C.H. SCHOLZ, K. SHIMAZAKI and T. MATSUDA (1984): Integration of geological and seismological data for the analysis of seismic hazard: a case study of Japan, *Bull. Seismol. Soc. Am.*, **74**, 687-708.

YEGULALP, T.M. and J.T. KUO (1974): Statistical prediction of occurrence of maximum magnitude earthquakes, *Bull. Seismol. Soc. Am.*, **64**, 393-414.

(received October 21, 1998;
accepted June 21, 1999)